PHYSICAL REVIEW D VOLUME 14, NUMBER 6 15 SEPTEMBER 1976

Flux tubes, monopoles, and the magnetic confinement of quarks*

H. W. Wyld
Department of Physics, University of Illinois, Urbana, Illinois 61801

R. T. Cutler
High Energy Physics Division, Argonne National Laboratory, Argonne, Illinois 60439

(Received 8 March 1976; revised manuscript received 25 June 1976)

A numerical study is made of the gauge-field model of magnetic confinement. The nonlinear differential equations describing a flux tube are solved by a relaxation method. Particular attention is paid to the boundary conditions at the center of the flux tube. We also study numerically the 't Hooft monopole and a flux tube of finite length, i.e., a quark-antiquark pair a finite distance apart.

I. INTRODUCTION

There is much current speculation aimed at devising a mechanism for quark confinement. Two general classes of models are studied, "electric" confinement and "magnetic" confinement, both based on gauge-field theories of a quark-gluon interaction. Although the electric confinement mechanism[1-3] is perhaps *a priori* the more plausible of the two, it is much more difficult to make it work, and at present this possibility is speculative. On the other hand, the magnetic confinement mechanism[4-13] does work, although one may be reluctant to accept the many assumptions made at the outset.

In the magnetic confinement models the quarks are endowed with a "magnetic" monopole moment, albeit in a color space or other space different from the flavor space which contains the usual electric and magnetic charges. There is also assumed a Higgs field which undergoes a spontaneous symmetry breakdown to provide the gauge bosons with a mass. The Higgs field has the usual type of electric coupling to the gauge field, i.e., there are no magnetic monopoles in the Higgs field. The magnetic flux produced by the quark magnetic monopoles is thus shielded by the Higgs field by a mechanism strictly analogous to the Meissner effect in a superconductor. The magnetic field produced by a quark monopole is channeled into a flux tube; a quark-antiquark pair is connected by such a flux tube. For appreciable separations of the quark-antiquark pair the energy of this flux tube is proportional to its length, and this is the desired confinement potential.

In the electric confinement models it is hoped that something similar happens: that the electric flux is confined to a flux tube by the infrared divergences and/or the nonlinear interactions of the gauge-field theory. We will have nothing more to say about electric confinement in the present paper.

The flux-tube mechanism of magnetic confinement was invented by Nielsen and Olesen,[4] Nambu,[5] and Parisi,[6] and has been developed in subsequent papers by 't Hooft,[7] Polyakov,[8] Mandelstam,[9] Eguchi,[10] Ezawa and Tze,[11] Corrigan *et al.*,[12] and many others. For the most part these papers deal with solutions of the field equations interpreted as classical c-number equations. An analytical approximation scheme has been given by Patkós.[13] Much of the work is a direct carryover from developments in the theory of superconductivity.[14]

In the present paper we attempt to clarify and illustrate the model by giving some numerical solutions for the classical field equations. The theory is reviewed and numerical results for the Abelian version of the model are given in Sec. II for the case of an infinitely long flux tube, i.e., the vortex tube of Nielsen and Olesen.[4] In Sec. III the numerical methods used in Sec. II are applied to the 't Hooft magnetic monopole[7]; the equations describing this non-Abelian soliton are rather similar to those studied in the preceding section. In Sec. IV we discuss briefly some attempts to carry out the numerical work for a flux tube of finite length, i.e., a quark-antiquark pair a finite distance apart.

The equations to be solved in this work are nonlinear differential equations with boundary conditions given at both $r=0$ and $r=\infty$. They are solved by the relaxation method of Henyey, Wilets, Böhm, LeLevier, and Levee,[15] which is widely employed by astrophysicists for solving the differential equations describing stellar structure.[16] This method would appear to be generally useful for obtaining numerically soliton-type solutions of classical nonlinear field equations. We devote an appendix to a brief discussion of the method and the experience we have with it for the problems discussed in this paper. The method has been used by Nohl[17] to solve a problem similar to those discussed here.

II. ABELIAN MODEL

We treat the magnetic monopole quarks as external sources and account for them through boundary consitions on the gauge fields and Higgs field. For the Abelian model the Lagrangian for the gauge field A_μ coupled to the scalar Higgs field Ψ is

$$\mathcal{L} = -\tfrac{1}{4}F_{\mu\nu}{}^2 - \left(\frac{\partial}{\partial x_\mu} - ieA_\mu\right)\Psi\left(\frac{\partial}{\partial x_\mu} + ieA_\mu\right)\Psi^* + \mu^2\Psi^*\Psi - \tfrac{1}{2}\lambda(\Psi^*\Psi)^2 \tag{2.1}$$

with

$$F_{\mu\nu} = \frac{\partial A_\nu}{\partial x_\mu} - \frac{\partial A_\mu}{\partial x_\nu}. \tag{2.2}$$

This leads to field equations

$$\frac{\partial F_{\mu\nu}}{\partial x_\nu} = -ie\left(\Psi^*\frac{\partial\Psi}{\partial x_\mu} - \frac{\partial\Psi^*}{\partial x_\mu}\Psi\right) - 2e^2A_\mu\Psi^*\Psi \tag{2.3}$$

and

$$\left(\frac{\partial}{\partial x_\mu} - ieA_\mu\right)^2\Psi = -\mu^2\Psi + \lambda(\Psi^*\Psi)\Psi. \tag{2.4}$$

For a time-independent magnetic solution, take $A_4 = 0$ and A_i $(i = 1, 2, 3)$ and Ψ independent of time. With

$$\vec{B} = \operatorname{curl}\vec{A} \tag{2.5}$$

the field equations (2.3) and (2.4) become

$$\operatorname{curl}\vec{B} = -ie[\Psi^*\nabla\Psi - (\nabla\Psi^*)\Psi] - 2e^2\vec{A}\Psi^*\Psi \tag{2.6}$$

and

$$(\nabla^2 - 2ie\vec{A}\cdot\nabla - e^2\vec{A}^2)\Psi = -\mu^2\Psi + \lambda(\Psi^*\Psi)\Psi, \tag{2.7}$$

provided the gauge is chosen so that

$$\operatorname{div}\vec{A} = 0. \tag{2.8}$$

For one or more magnetic monopoles along the z axis, take

$$\vec{A} = \hat{\phi}A(\rho, z), \tag{2.9}$$

$$\Psi = e^{im\phi}\psi(\rho, z), \quad m = \text{integer}, \tag{2.10}$$

where $\hat{\phi}$ is a unit vector in the ϕ direction, ρ, ϕ, z are the usual cylindrical coordinates, and $\psi(\rho, z)$ is a real function. With these assumptions (2.8) is satisfied and the field equations (2.6) and (2.7) reduce to

$$\frac{\partial^2 A}{\partial z^2} + \frac{\partial^2 A}{\partial\rho^2} + \frac{1}{\rho}\frac{\partial A}{\partial\rho} - \frac{1}{\rho^2}A = 2e^2\left(A - \frac{m}{e\rho}\right)\psi^2, \tag{2.11}$$

$$\frac{\partial^2\psi}{\partial z^2} + \frac{\partial^2\psi}{\partial\rho^2} + \frac{1}{\rho}\frac{\partial\psi}{\partial\rho} = e^2\psi\left(A - \frac{m}{e\rho}\right)^2 - \mu^2\psi + \lambda\psi^3. \tag{2.12}$$

If the only sources are magnetic monopoles of opposite sign at $z = \pm\infty$, A and ψ are independent of z, and we have the vortex tube of Nielsen and Olesen. For this case the coupled differential equations are ordinary differential equations:

$$\frac{d^2A}{d\rho^2} + \frac{1}{\rho}\frac{dA}{d\rho} - \frac{1}{\rho^2}A = 2e^2\left(A - \frac{m}{e\rho}\right)\psi^2, \tag{2.13}$$

$$\frac{d^2\psi}{d\rho^2} + \frac{1}{\rho}\frac{d\psi}{d\rho} = e^2\left(A - \frac{m}{e\rho}\right)^2\psi - \mu^2\psi + \lambda\psi^3. \tag{2.14}$$

In addition to (2.13) and (2.14) we need boundary conditions. For the vortex tube the appropriate conditions are

$$\rho \to \infty: \quad \psi \to (\mu^2/\lambda)^{1/2}, \tag{2.15}$$

$$A \to m/e\rho, \tag{2.16}$$

$$\rho \to 0: \quad \psi \to a\rho^m, \tag{2.17}$$

$$A \to b\rho, \tag{2.18}$$

with a and b unknown constant. In (2.15) we assume for $\rho \to \infty$ the usual symmetry-breakdown value for the Higgs field. If this value is substituted on the right of Eq. (2.13) we obtain a form of Bessel's equation for $A_1 = A - m/e\rho$. [Note that $m/e\rho$ is a pure gauge field and reduces the left side of (2.13) to zero.] One solution of the Bessel equation grows exponentially with ρ and is rejected. The other decays exponentially, leading to the boundary condition (2.16).

To obtain the boundary conditions (2.17) and (2.18) at $\rho \to 0$, first note that the flux through a circle of radius ρ centered on the flux tube is given by

$$\Phi(\rho) = \int \operatorname{curl}\vec{A}\cdot d\vec{s} = \oint \vec{A}\cdot d\vec{l} = 2\pi\rho A(\rho). \tag{2.19}$$

If we assume that $\Phi(\rho) \to 0$ as $\rho \to 0$, thus for example eliminating a Dirac string at $\rho = 0$, we see that $A(\rho)$ is less singular than ρ^{-1} at $\rho \to 0$. The leading terms in (2.14) for small ρ are then

$$\frac{d^2\psi}{d\rho^2} + \frac{1}{\rho}\frac{d\psi}{d\rho} - \frac{m^2}{\rho^2}\psi = 0. \tag{2.20}$$

This has solutions $\rho^{\pm m}$. Eliminating the singular solution leads to the boundary condition (2.17). The leading terms in (2.13) at small ρ are then

$$\frac{d^2A}{d\rho^2} + \frac{1}{\rho}\frac{dA}{d\rho} - \frac{1}{\rho^2}A = 0 \tag{2.21}$$

with solutions $\rho^{\pm 1}$. The condition that A be less singular than ρ^{-1} then leads to the boundary condition (2.18).

The integer m is the number of flux quanta in the flux tube. According to (2.19) for $\rho \to \infty$ and (2.16) we find for the total flux

$$\Phi = \frac{2\pi m}{e}. \tag{2.22}$$

In terms of the magnetic monopole moment g of the monopoles at the end of the flux tube, the total flux is $\Phi = g$ (in rationalized units), so we have the Dirac quantization condition

$$eg = 2\pi m. \tag{2.23}$$

The energy per unit length of the flux tube relative to the Higgs vacuum is given by

$$\frac{E}{L} = 2\pi \int_0^\infty \rho\, d\rho \left\{ \left(\frac{\partial \psi}{\partial \rho}\right)^2 + e^2\psi^2\left(A - \frac{m}{e\rho}\right)^2 + \frac{1}{2}\left[\frac{1}{\rho}\frac{\partial}{\partial \rho}(\rho A)\right]^2 - \mu^2\psi^2 + \tfrac{1}{2}\lambda\psi^4 + \frac{\mu^4}{2\lambda}\right\}. \tag{2.24}$$

Eliminating the derivatives in this expression by integrating by parts and using the field equations (2.13) and (2.14), we find

$$\frac{E}{L} = \frac{\pi}{e}B(0) + 2\pi \int_0^\infty \rho\, d\rho \left[-e^2\psi^2\left(A - \frac{m}{e\rho}\right)^2 - \frac{\lambda}{2}\left(\psi^4 - \frac{\mu^4}{\lambda^2}\right)\right], \tag{2.25}$$

where the magnetic field is given by

$$B(\rho) = \frac{1}{\rho}\frac{d}{d\rho}(\rho A). \tag{2.26}$$

For numerical purposes it is convenient to introduce dimensionless variables. The masses of the scalar and vector mesons after the spontaneous symmetry breakdown are

$$m_s = (2\mu^2)^{1/2}, \tag{2.27}$$

$$m_V = \left(\frac{2e^2\mu^2}{\lambda}\right)^{1/2}. \tag{2.28}$$

Introduce a dimensionless length ρ',

$$\rho = \frac{1}{m_V}\rho', \tag{2.29}$$

and dimensionless scalar and vector fields ψ', A',

$$\psi = \left(\frac{\mu^2}{\lambda}\right)^{1/2}\psi', \tag{2.30}$$

$$A = \frac{m_V}{e}A'. \tag{2.31}$$

In terms of these variables there is a dimensionless coupling constant

$$G = \frac{\lambda}{e^2} = \frac{m_s^2}{m_V^2}. \tag{2.32}$$

The field equations (2.13) and (2.14) in terms of dimensionless variables become (dropping primes)

$$\frac{d^2A}{d\rho^2} + \frac{1}{\rho}\frac{dA}{d\rho} - \frac{1}{\rho^2}A = \psi^2\left(A - \frac{m}{\rho}\right), \tag{2.33}$$

$$\frac{d^2\psi}{d\rho^2} + \frac{1}{\rho}\frac{d\psi}{d\rho} = \psi\left(A - \frac{m}{\rho}\right)^2 - \tfrac{1}{2}G(\psi - \psi^3), \tag{2.34}$$

with boundary conditions

$$\rho \to \infty:\ \psi \to 1, \quad A \to m/\rho, \tag{2.35}$$

$$\rho \to 0:\ \psi \to a\rho^m, \quad A \to b\rho, \tag{2.36}$$

and the energy per unit length (2.25) becomes

$$\frac{E}{L} = \pi\frac{m_V^2}{e^2}f(G), \tag{2.37}$$

$$f(G) = B(0) + C,$$
$$C = \int_0^\infty \rho\, d\rho\left[-\psi^2\left(A - \frac{m}{\rho}\right)^2 + \tfrac{1}{4}G(1 - \psi^4)\right], \tag{2.38}$$

with

$$B(\rho) = \frac{1}{\rho}\frac{d}{d\rho}(\rho A). \tag{2.39}$$

Some numerical results for the equations (2.33)–(2.39) for the case $m = 1$ (one unit of flux) are presented in Figs. 1, 2, and 3. These results were obtained with the relaxation method discussed in the Appendix. Figure 1 presents $B(\rho)$ as a function of ρ for various values of G, ranging from weak coupling ($G = 0.1$) to strong coupling ($G = 100.0$). Corresponding results for the Higgs

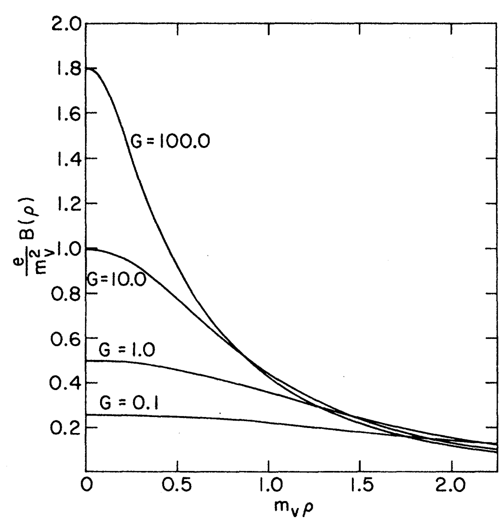

FIG. 1. The magnetic field $B(\rho)$ as a function of radius in the Abelian model with $m = 1$ (1 unit of flux) for several values of the coupling parameter $G = \lambda/e^2$. $m_V^2 = 2e^2\mu^2/\lambda$.

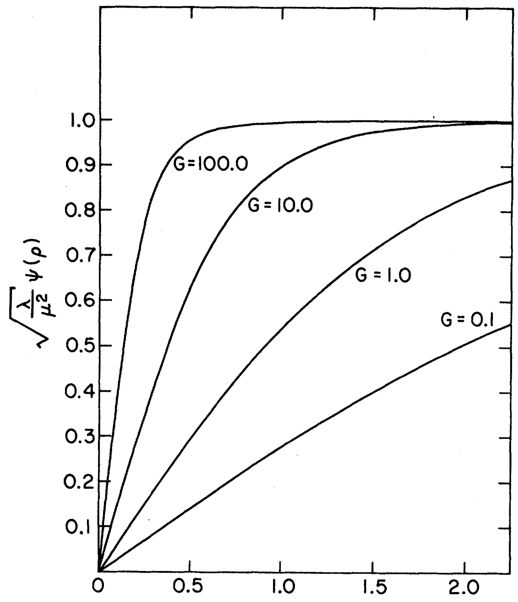

FIG. 2. The Higgs field $\psi(\rho)$ as a function of radius in the Abelian model with $m=1$ (1 unit of flux) for several values of the coupling parameter $G=\lambda/e^2$. $m_V{}^2=2e^2\mu^2/\lambda$.

field $\psi(\rho)$ are presented in Fig. 2. For strong coupling ψ maintains its asymptotic value outside of a narrow core. This is the basis of an approximation technique in which ψ is replaced by its asymptotic value in Eq. (2.13)—see for example Ref. 13. In Fig. 3 we give $B(0)$, the magnetic field at the center of the flux tube, as a function of the coupling parameter G. Also plotted in Fig. 3 is the quantity $f(G)=B(0)+C$, which is directly proportional to the energy per unit length of the flux tube. We see that these quantities are very slowly

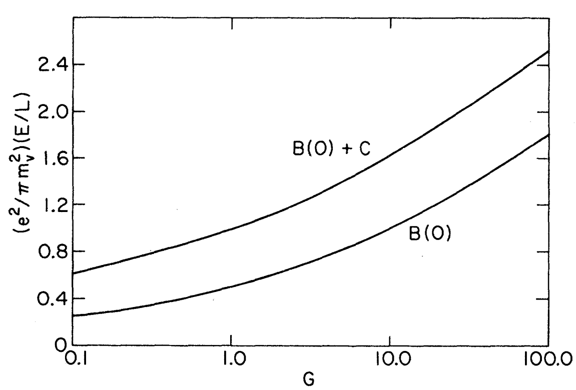

FIG. 3. The energy per unit length of the flux tube in the Abelian model with $m=1$ (1 unit of flux) as a function of the coupling parameter $G=\lambda/e^2$. The quantities $B(0)$ and $B(0)+C$ are plotted—see Eqs. (2.37) and (2.38). $m_V{}^2=2e^2\mu^2/\lambda$.

varying functions of G.

We can attempt to attach some physical significance to these numerical values by comparison with phenomenological potentials used in recent studies of charmonium spectroscopy. Eichten *et al.*[18] use a potential

$$V(r)=-\frac{\alpha_s}{r}\left[1-\left(\frac{r}{a}\right)^2\right] \qquad (2.40)$$

and find that the values $\alpha_s=0.2$, $a=0.2$ fm, fit the data. The Coulomb potential part of (2.40) determines the monopole strength g and hence the gauge coupling constant by (2.23):

$$\alpha_s=0.2=\frac{g^2}{4\pi}=\frac{\pi}{e^2}, \quad \frac{e^2}{4\pi}=1.25. \qquad (2.41)$$

The linear term in the potential (2.40) is the energy per unit length we have calculated, (2.37) and (2.38):

$$\pi\frac{m_V{}^2}{e^2}f(G)=\frac{\alpha_s}{a^2}=\frac{0.2}{(0.2\text{ fm})^2}=10m_\pi{}^2,$$
$$m_V{}^2=\frac{10e^2}{\pi}m_\pi{}^2\frac{1}{f(G)}. \qquad (2.42)$$

With e given by (2.41), the vector-meson mass is given by (2.42). The parameter G is not fixed by these considerations, but $f(G)$ is a slowly varying function. Using the value (2.41) for e and the curve in Fig. 3, we calculated the scalar Higgs meson and vector-meson masses for typical values of G, as given in Table I.

III. THE 't HOOFT MONOPOLE

The numerical technique employed in Sec. II to solve the nonlinear coupled differential equations with boundary conditions at $\rho=0$ and $\rho=\infty$ describing the Nielsen-Olesen vortex is a generally useful technique for calculating numerically soliton solutions of nonlinear classical field equations. In this section we discuss the 't Hooft monopole,[7] which is described by nonlinear coupled differential equations similar to those for the Nielsen-Olesen vortex.

The 't Hooft monopole is a soliton solution of the field equations for a system consisting of an SU(2)

TABLE I. Some numerical values given by the formulas (2.41) and (2.42).

G	$f(G)$	m_V (GeV)	$m_S=\sqrt{G}m_V$ (GeV)
0.1	0.610	1.28	0.40
1.0	0.975	1.01	1.01
10.0	1.626	0.78	2.47
100.0	2.53	0.63	6.30

isovector gauge field A_μ^a, $a=1,2,3$, and an isovector Higgs field Ψ^a. In terms of the covariant derivatives

$$F_{\mu\nu}^a=\frac{\partial A_\nu^a}{\partial x_\mu}-\frac{\partial A_\mu^a}{\partial x_\nu}+e\epsilon_{abc}A_\mu^b A_\nu^c \tag{3.1}$$

and

$$D_\mu \Psi^a=\frac{\partial \Psi^a}{\partial x_\mu}+e\epsilon_{abc}A_\mu^b\Psi^c \tag{3.2}$$

the Lagrangian is

$$\mathcal{L}=-\tfrac{1}{4}(F_{\mu\nu}^a)^2-\tfrac{1}{2}(D_\mu\Psi^a)^2+\tfrac{1}{2}\mu^2(\Psi^a)^2-\tfrac{1}{4}\lambda[(\Psi^a)^2]^2. \tag{3.3}$$

't Hooft discovered that the field equation for this model, i.e.,

$$D_\nu F_{\mu\nu}^a-e\epsilon_{abc}(D_\mu\Psi^b)\Psi^c=0 \tag{3.4}$$

and

$$D_\mu{}^2\Psi^a+\mu^2\Psi^a-\lambda\Psi^a(\Psi^b)^2=0\,, \tag{3.5}$$

have a time-independent spherically symmetric solution with the tensor form

$$A_\mu^a=-\epsilon_{\mu ab}\frac{x_b}{r}F(r),\quad \mu=1,2,3;\quad A_4^a=0\,, \tag{3.6}$$

$$\Psi^a=\frac{x_a}{r}\chi(r)\,. \tag{3.7}$$

Substituting (3.6) and (3.7) in (3.4) and (3.5) one obtains coupled nonlinear differential equations for $F(r)$ and $\chi(r)$. Introducing dimensionless variables

$$r=\frac{1}{m_V}r',\quad m_V{}^2=\frac{\mu^2e^2}{\lambda},\quad F=\left(\frac{\mu^2}{\lambda}\right)^{1/2}F',\quad \chi=\left(\frac{\mu^2}{\lambda}\right)^{1/2}\chi',\quad G=\frac{\lambda}{e^2}, \tag{3.8}$$

we find (dropping primes)

$$\frac{d^2F}{dr^2}+\frac{2}{r}\frac{dF}{dr}+\left(F-\frac{1}{r}\right)\left[-\left(F-\frac{1}{r}\right)^2+\frac{1}{r^2}-\chi^2\right]=0\,, \tag{3.9}$$

$$\frac{d^2\chi}{dr^2}+\frac{2}{r}\frac{d\chi}{dr}-2\left(F-\frac{1}{r}\right)^2\chi+G\chi(1-\chi^2)=0\,. \tag{3.10}$$

The appropriate boundary conditions to be applied in solving these equations are

$$r\to\infty:\ \chi\to 1\,, \tag{3.11}$$

$$F\to 1/r\,, \tag{3.12}$$

$$r\to 0:\ \chi\to ar\,, \tag{3.13}$$

$$F\to br\,, \tag{3.14}$$

with a and b unknown constants. To check (3.11) and (3.12) substitute $\chi=1+\delta\chi$, $F=1/r+\delta F$ in (3.9) and (3.10) and linearize in $\delta\chi, \delta F$. The resulting linear equations have exponential-type solutions for $r\to\infty$. Eliminating the exponentially growing solutions, we are left with solutions in which δF and $\delta\chi$ approach zero exponentially as $r\to\infty$. To obtain (3.13) and (3.14) assume power series solutions for (3.9) and (3.10) near $r\to 0$. The indicial equations determine the variations near the origin. Eliminating singular solutions in which χ and F vary as r^{-2} near $r\to 0$, we find the linearly varying solutions (3.13) and (3.14).

For a time-independent solution the energy is the negative of the space integral of the Lagrange density (3.3). Substituting (3.6) and (3.7) in this formula, integrating by parts, and using (3.9) and (3.10) to eliminate derivatives, we find for the energy the expression (in dimensionless variables)

$$E=4\pi\frac{m_V}{e^2}\int_0^\infty dr\,r^2\left\{-\tfrac{1}{2}F^4(r)+\frac{1}{r}F^3(r)-F(r)\left[F(r)-\frac{1}{r}\right]\chi^2(r)+\tfrac{1}{4}G[1-\chi^4(r)]\right\}. \tag{3.15}$$

Numerical results for Eqs. (3.9)–(3.15), obtained by the relaxation method discussed in the

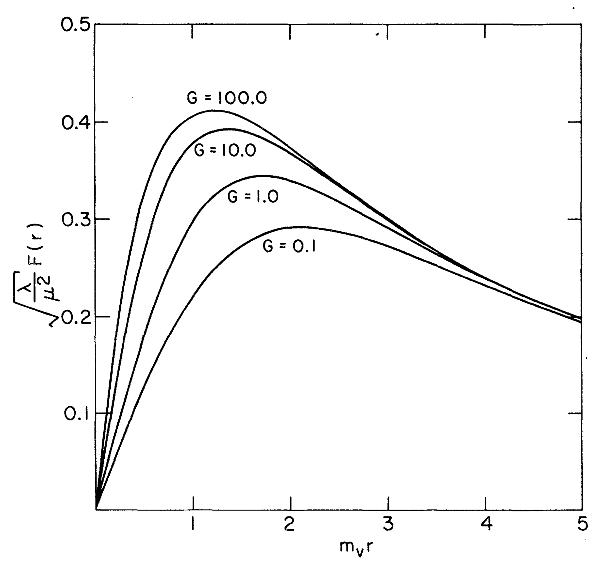

FIG. 4. The vector field $F(r)$ as a function of radius in the 't Hooft model of the magnetic monopole for several values of the coupling parameter $G=\lambda/e^2$. $m_V{}^2=e^2\mu^2/\lambda$.

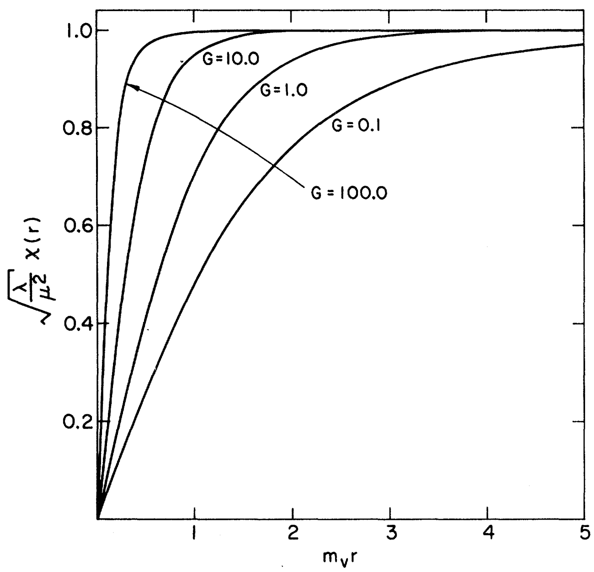

FIG. 5. The Higgs field $\chi(r)$ as a function of radius in the 't Hooft model of the magnetic monopole for several values of the coupling parameter $G=\lambda/e^2$. $m_V{}^2=e^2\mu^2/\lambda$.

Appendix, are given in Figs. 4, 5, and 6. Figure 4 presents $F(r)$ as a function of r for various values of the dimensionless coupling parameter $G=\lambda/e^2$. The corresponding results for the Higgs field $\chi(r)$ are given in Fig. 5. As for the vortex solutions of Sec. II, for strong coupling, $G\gg 1$, $\chi(r)$ differs from its asymptotic value only in a narrow core. In Fig. 6 we give the energy of the monopole as a function of G. It is a very slowly varying function. Our numerical values are nearly, but not quite, in agreement with those obtained by 't Hooft[7] using a variational technique.

IV. DIPOLE CALCULATIONS

In this section we consider the solution of the Eqs. (2.11) and (2.12) for a dipole consisting of positive and negative magnetic monopoles ($\pm g$) a distance $2b$ apart— see Fig. 7. First we remind the reader of the vector potential for magnetic monopoles and dipoles in the absence of the Higgs field. For a single monopole g located at the origin the vector potential (in spherical coordinates)

$$A_\phi=-\frac{g}{4\pi r}\frac{\sin\theta}{1-\cos\theta}\,,\quad A_\theta=A_r=0\,, \tag{4.1}$$

gives a Coulomb field

$$B_r=\mathrm{curl}_r\vec{A}=\frac{g}{4\pi r^2}\,,\quad B_\theta=B_\phi=0\,. \tag{4.2}$$

The direction of the Dirac string is arbitrary. In (4.1) it lies along the line $\cos\theta=1$. For the dipole of Fig. 7 we have

$$\begin{aligned}A_\phi&=-\frac{g}{4\pi}\left[\frac{\sin\theta_1}{r_1(1-\cos\theta_1)}-\frac{\sin\theta_2}{r_2(1-\cos\theta_2)}\right]\\&=-\frac{g}{2\pi b}\frac{(1-\eta^2)^{1/2}}{(\xi^2-1)^{1/2}}\frac{\xi}{(\xi^2-\eta^2)}\\&=-\frac{1}{eb}\frac{(1-\eta^2)^{1/2}}{(\xi^2-1)^{1/2}}\frac{\xi}{(\xi^2-\eta^2)}\,.\end{aligned} \tag{4.3}$$

Here we have introduced elliptic coordinates

$$\xi=\frac{r_1+r_2}{2b}\,,\quad \eta=\frac{r_1-r_2}{2b}\,, \tag{4.4}$$

$$\rho=b[(\xi^2-1)(1-\eta^2)]^{1/2}\,,\quad z=b\xi\eta\,, \tag{4.5}$$

and have used the quantization condition (2.23), assuming that $m=1$.

We now transform to elliptic coordinates in (2.11) and (2.12). Take $m=1$ in those equations

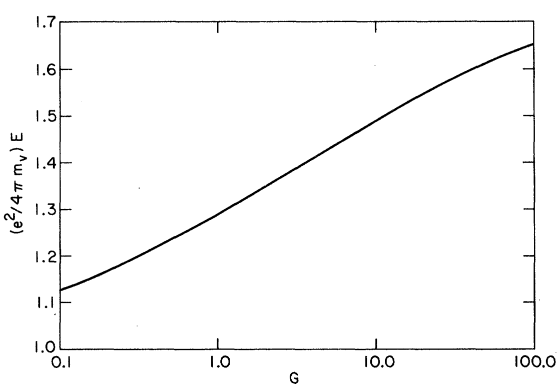

FIG. 6. Energy of the monopole in the 't Hooft model as a function of the coupling parameter $G=\lambda/e^2$. $m_V{}^2=e^2\mu^2/\lambda$.

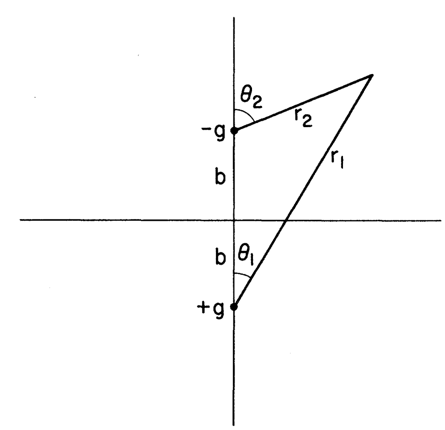

FIG. 7. Geometric quantities for the magnetic dipole. Monopoles of strength ($\pm g$) are separated by a distance $2b$.

and use as dependent variable

$$A_1 = A - \frac{1}{e\rho}. \quad (4.6)$$

Further, introducing dimensionless variables ψ', A_1',

$$\psi = \left(\frac{\mu^2}{\lambda}\right)^{1/2} \psi', \qquad A_1 = \frac{1}{eb} A_1' \quad (4.7)$$

and dropping the primes we obtain in place of (2.11) and (2.12)

$$\frac{1}{\xi^2-\eta^2}\left\{\frac{\partial}{\partial \xi}\left[(\xi^2-1)\frac{\partial A_1}{\partial \xi}\right] + \frac{\partial}{\partial \eta}\left[(1-\eta^2)\frac{\partial A_1}{\partial \eta}\right] - \frac{\xi^2-\eta^2}{(\xi^2-1)(1-\eta^2)}A_1\right\} = R^2\psi^2 A_1, \quad (4.8)$$

$$\frac{1}{\xi^2-\eta^2}\left\{\frac{\partial}{\partial \xi}\left[(\xi^2-1)\frac{\partial \psi}{\partial \xi}\right] + \frac{\partial}{\partial \eta}\left[(1-\eta^2)\frac{\partial \psi}{\partial \eta}\right]\right\} = \psi A_1{}^2 - \tfrac{1}{2}GR^2(\psi-\psi^3). \quad (4.9)$$

There are two dimensionless parameters in these equations, $R = m_V b$ and G, with m_V given by (2.28) and G by (2.32).

A convenient way to incorporate the boundary conditions on A_1 is to factor out the dipole form (4.3). Thus we write (in dimensionless variables)

$$A_1 = -\frac{(1-\eta^2)^{1/2}}{(\xi^2-1)^{1/2}}\,\frac{\xi}{\xi^2-\eta^2}F(\xi,\eta). \quad (4.10)$$

The boundary conditions are now

$$\xi \to \infty:\ F(\xi,\eta) \to 0, \quad (4.11)$$

$$\psi(\xi,\eta) \to 1, \quad (4.12)$$

$$\xi \to 1:\ F(\xi,\eta) \to 1, \quad (4.13)$$

$$\psi(\xi,\eta) \to 0. \quad (4.14)$$

Actually, the relaxation method of solving the differential equations will not converge unless one specifies the manner of variation near the singular line $\xi \to 1$, particularly near the singular points $\xi \to 1$, $\eta \to \pm 1$, where the monopoles are located—this was also necessary in the one-dimensional case; see (2.17), (2.18), and (A19). It is also convenient to spread out these singular regions by a change of variables

$$x = (\xi^2-1)^{1/2}, \quad y = (1-\eta^2)^{1/2}, \quad (4.15)$$

such that

$$\begin{aligned} &\rho = bx, \quad |z| = 0 \text{ when } y = 1, \\ &\rho = 0, \quad |z| = b(1+x^2)^{1/2} \text{ when } y = 0, \\ &\rho = 0, \quad |z| = b(1-y^2)^{1/2} \text{ when } x = 0, \\ &\rho = bxy, \quad |z| = bx(1-y^2)^{1/2} \text{ when } x \to \infty. \end{aligned} \quad (4.16)$$

In terms of these variables, Eqs. (4.8) and (4.9) become

$$(x^2+1)\frac{\partial^2 F}{\partial x^2} - \left[\frac{1}{x} + \frac{2x(2+x^2-y^2)}{x^2+y^2}\right]\frac{\partial F}{\partial x} + (1-y^2)\frac{\partial^2 F}{\partial y^2} + \left(-\frac{1}{y} + \frac{4x^2}{x^2+y^2}\,\frac{1-y^2}{y}\right)\frac{\partial F}{\partial y} = (x^2+y^2)R^2\psi^2 F, \quad (4.17)$$

$$(x^2+1)\frac{\partial^2 \psi}{\partial x^2} + \left(2x + \frac{1}{x}\right)\frac{\partial \psi}{\partial x} + (1-y^2)\frac{\partial^2 \psi}{\partial y^2} + \left(-2y + \frac{1}{y}\right)\frac{\partial \psi}{\partial y} = \frac{x^2+1}{x^2}\,\frac{y^2}{x^2+y^2}F^2\psi - \tfrac{1}{2}GR^2(x^2+y^2)(\psi-\psi^3). \quad (4.18)$$

For x and y both small the leading terms in these equations are

$$xy(x^2+y^2)\left(\frac{\partial^2 F}{\partial x^2} + \frac{\partial^2 F}{\partial y^2}\right) - [y(x^2+y^2) + 4x^2y]\frac{\partial F}{\partial x} + [-x(x^2+y^2) + 4x^3]\frac{\partial F}{\partial y} = 0, \quad (4.19)$$

$$x^2y^2(x^2+y^2)\left(\frac{\partial^2 \psi}{\partial x^2} + \frac{\partial^2 \psi}{\partial y^2}\right) + xy(x^2+y^2)\left(y\frac{\partial \psi}{\partial x} + x\frac{\partial \psi}{\partial y}\right) = y^4\psi, \quad (4.20)$$

and the solutions of these satisfying the boundary conditions (4.13) and (4.14) are

$$x, y \to 0:\ F \to 1 - cx^2(x^2+y^2), \quad (4.21)$$

$$\psi \to ax(x^2+y^2)^\alpha, \quad \alpha = -1 + \tfrac{1}{2}\sqrt{3}, \quad (4.22)$$

with a and c unknown constants. These are the boundary conditions for both x and y small. For only x small we have

$$x \to 0:\ F \to 1 - f(y)x^2, \quad (4.23)$$

$$\psi \to d(y)x, \quad (4.24)$$

with $d(y)$ and $f(y)$ unknown functions of y.

The constant c in (4.21), which must be evaluated in the course of the numerical solution of the differential equations, is closely related to the force between the monopole-antimonopole pair. The ξ component of the magnetic field is

$$B_\xi = \frac{-1}{eb^2}\frac{1}{(\xi^2-\eta^2)^{1/2}}\frac{\partial}{\partial\eta}[(1-\eta^2)^{1/2}A_1]$$

$$= \frac{1}{eb^2}\frac{1}{(\xi^2-\eta^2)^{1/2}}\frac{\xi}{(\xi^2-1)^{1/2}}\frac{\partial}{\partial\eta}\left[\frac{1-\eta^2}{\xi^2-\eta^2}F(\xi,\eta)\right]. \quad (4.25)$$

Along the line $\eta=1$, above the monopole $(-g)$ (see Fig. 7), this reduces to

$$B_\xi = -\frac{2}{eb^2}\frac{\xi}{(\xi^2-1)^2}F(\xi,1). \quad (4.26)$$

Subtracting out the self-field of the monopole $(-g)$,

$$B_\xi^{\text{self}} = \frac{-1}{2eb^2}\frac{1}{(\xi-1)^2}, \quad (4.27)$$

we find for the field due to the monopole $(+g)$ and the surrounding Higgs field

$$B_\xi - B_\xi^{\text{self}} = \frac{1}{2eb^2}\frac{1}{(\xi-1)^2}\left[1-\frac{4\xi}{(\xi+1)^2}F(\xi,1)\right] \quad (4.28)$$

along the line $\eta=1$. The limit of this expression as we approach the location $\xi=1$ of the monopole $(-g)$ is

$$B_\xi - B_\xi^{\text{self}} \xrightarrow[\xi\to1]{} \frac{1}{8eb^2}\left[1-2\frac{\partial^2F(\xi,1)}{\partial\xi^2}\bigg|_{\xi=1}\right]$$

$$= \frac{1}{8eb^2}\left(1-\frac{2}{3}\frac{\partial^4F}{\partial x^4}\bigg|_{x=0}\right)$$

$$= \frac{1}{8eb^2}(1+16c), \quad (4.29)$$

in terms of the constant c in (4.21).

We can also use the formula for B_η,

$$B_\eta = \frac{1}{eb^2}\frac{(1-\eta^2)^{1/2}}{(\xi^2-\eta^2)^{3/2}}\left(\frac{\xi^2+\eta^2}{\xi^2-\eta^2}F-\xi\frac{\partial F}{\partial\xi}\right), \quad (4.30)$$

which, along the line $\xi=1$, below the monopole $(-g)$, yields

$$B_\eta = \frac{1}{eb^2}\frac{1}{(1-\eta^2)}\left(\frac{1+\eta^2}{1-\eta^2}-\frac{\partial F}{\partial\xi}\bigg|_{\xi=1}\right). \quad (4.31)$$

Subtracting out the self-field,

$$B_\eta - B_\eta^{\text{self}} = \frac{1}{eb^2}\left[\frac{1}{2(1+\eta)^2}-\frac{1}{(1-\eta^2)}\frac{\partial F}{\partial\xi}\bigg|_{\xi=1}\right]$$

$$= \frac{1}{eb^2}\left[\frac{1}{2(1+\eta)^2}-\frac{1}{y^2}\frac{\partial^2F}{\partial x^2}\bigg|_{x=0}\right], \quad (4.32)$$

we obtain again

$$B_\eta - B_\eta^{\text{self}} \xrightarrow[\eta\to1]{} \frac{1}{8eb^2}(1+16c). \quad (4.33)$$

The force between the monopoles is thus

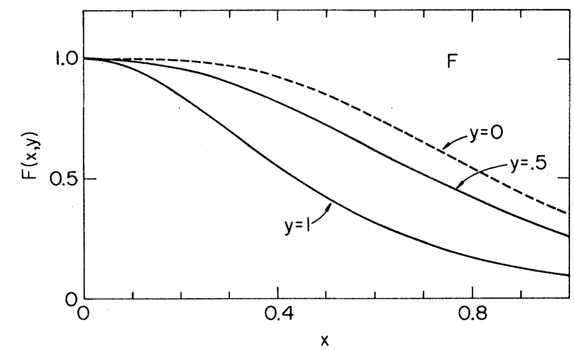

FIG. 8. The vector field $F(x,y)$ as a function of x for three values of y in the Abelian model of the dipole with $G=\lambda/e^2=2.0$, $R=m_V b=4.0$.

$$\text{force} = -g(B-B^{\text{self}})$$

$$= -\frac{g^2}{4\pi}\frac{1}{(2b)^2}(1+16c), \quad (4.34)$$

where we have used the quantization condition (2.23) with $m=1$. In (4.34), the force is given as the sum of the Coulomb force between the monopoles and a correction due to the shielding effect which produces the flux tube. For large separations $2b$ the contribution involving c in (4.34) should reduce to the energy per unit length calculated in Sec. II, Eq. (2.24) or Eq. (2.37).

In Figs. 8 and 9 we plot the fields $F(x,y)$ and $\psi(x,y)$ obtained with $G=2$ and $R=4$. The fields are slowly varying in y; the relaxation method discussed in the Appendix would be impractical if this were not so. Figure 10 shows the magnetic field (4.30) in the midplane of the dipole ($y=1$) for $G=2$ and various values of R. The formation of the flux tube discussed in Sec. II appears to be essentially complete for $R=4$, as evidenced by the fact that $B(0)$ approaches its asymptotic value and $B(x)$ approaches its proper shape.

The quantity $B-B^{\text{self}}$ is evaluated for $G=2$ at the

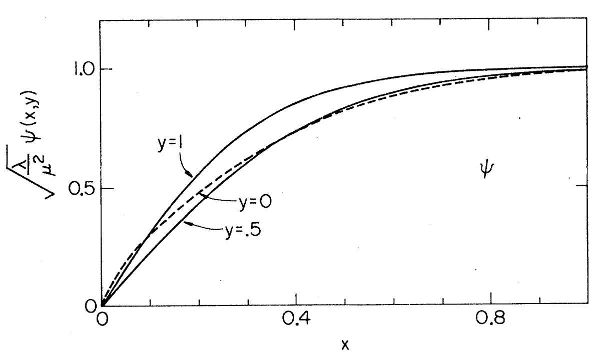

FIG. 9. The Higgs field $\psi(x,y)$ as a function of x for three values of y in the Abelian model of the dipole with $G=\lambda/e^2=2.0$, $R=m_V b=4.0$.

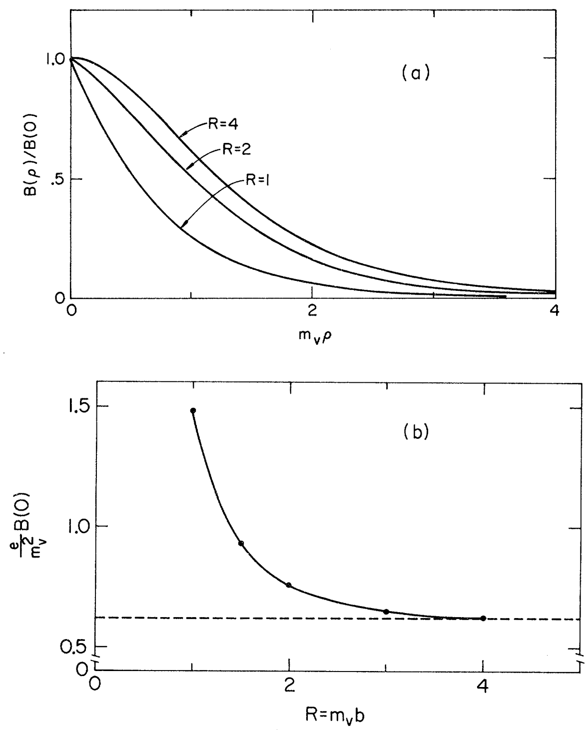

FIG. 10. The magnetic field $B(\rho)$ in the midplane of the dipole, $y=1$, for $G=\lambda/e^2=2.0$ and various values of $R=m_V b$. (a) $B(\rho)/B(0)$ as a function of ρ; (b) $B(0)$ as a function of R. The value of $B(0)$ for the infinite vortex of Sec. II is shown as a dashed line.

location of the monopole $(-g)$, Eq. (4.29), and is displayed in Fig. 11 as a function of R, the separation of the monopoles in dimensionless units. The force between the monopoles is proportional (Eq. 4.34) to the quantity plotted, and the result from Sec. II for this force (valid in the limit $R\to\infty$) is shown as a dashed line. The calculated force

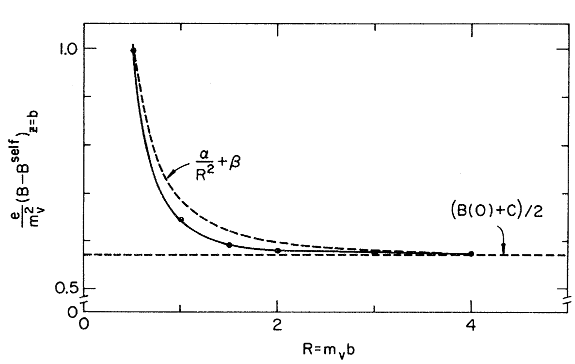

FIG. 11. B-B^{self} at the location of the monopole ($x=y=0$) for $G=\lambda/e^2=2.0$ as a function of $R=m_V b$. Shown as dashed lines are $[B(0)+C]/2$ from Sec. II, and $\beta+\alpha/R^2$. The values of α and β are chosen so that the two curves coincide at $R=0.25$ (not plotted) and $R=4.0$.

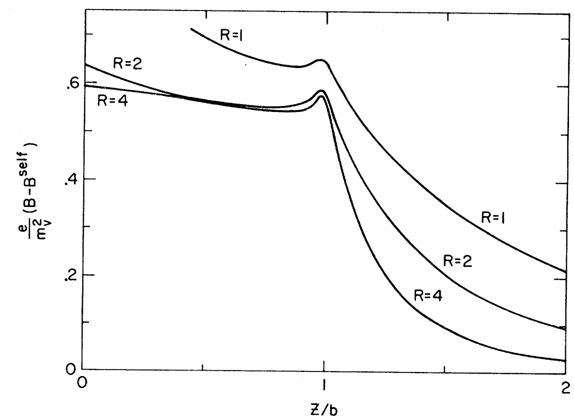

FIG. 12. $B-B^{\text{self}}$ along the z axis for $G=\lambda/e^2=2.0$ and several values of $R=m_V b$.

is very near its asymptotic value for $R\gtrsim 2$. Also plotted is a curve of the form $\beta+\alpha/R^2$, which is consistent with the commonly used phenomenological potential Eq. (2.40). The force between the dipoles for $G=2$ is somewhat different from this form in the intermediate region $R\cong 1$. A different choice of G would change the shape of this curve; there probably exists some value of G which results in a potential almost identical to the phenomenological form (2.40).

The magnetic field $B-B^{\text{self}}$ was calculated along the z axis, Eq. (4.16), using (4.28) for $z/b\geq 1$ and (4.32) for $z/b\leq 1$, and the results are shown in Fig. 12 for three values of R. We remind the reader that only the self-field of the monopole $(-g)$ at $z/b=+1$ has been subtracted out; the quantity $B-B^{\text{self}}$ is singular at $z/b=-1$. There were some numerical difficulties encountered in the evaluation of $d^2F/dx^2|_{x=0}$ in (4.32) which caused scatter on the 3–5% level in the values of $B-B^{\text{self}}$ calculated for $z/b\leq 1$; the curve drawn has been smoothed by eye. However, we are confident that such features as the bump near $z/b=1$ are not spurious, although the width and height of this structure are not well determined. A completely satisfactory solution to this problem (as well as a resolution of the difficulty discussed in the Appendix) would probably involve the use of a significantly more sophisticated numerical technique.[19] However, the physical interest of such fine details of the particular model discussed here did not seem sufficient to warrant the extra effort at this time.

ACKNOWLEDGMENTS

We would like to acknowledge helpful discussions about numerical methods with Professor I. Iben.

$$L_3 = -B_2^{-1}D_2, \quad K_3 = -B_2^{-1}Q_2 \ , \tag{A16}$$

and the M^2+M components of L_3 and K_3 can be computed and saved for future reference. Similarly, $\delta\phi_3$ can be expressed in terms of $\delta\phi_4$, and, in general,

$$\delta\phi_j = L_{j+1}\delta\phi_{j+1} + K_{j+1} \ , \tag{A17}$$

$$\begin{aligned} L_{j+1} &= -(B_j + C_jL_j)^{-1}D_j \ , \\ K_{j+1} &= -(B_j + C_jL_j)^{-1}(Q_j + C_jK_j) \ . \end{aligned} \tag{A18}$$

These recursion relations are used to calculate and store L_j and K_j for $j = 3, 4, \ldots, N$. However, at this point we know that $\delta\phi_N = 0$, and thus that (A17), (A9), and (A4) can be used to compute $\delta\phi_j$, ϕ_j, and Q_j for $j = N-1, N-2, \ldots, 2$. This should represent an improved solution, in the sense that $Q_j = 0$ should be more nearly satisfied for the new ϕ_j than it was for $\tilde{\phi}_j$. If all the values of Q_j are not satisfactorily small, ϕ_j can be used as a starting point for another relaxation.

If it converges at all, this iterative method usually converges extremely rapidly, requiring only a few iterations even if the initial guess is very bad. However, the singular points of the equation must be treated carefully. If $x_L = 0$ is such a point, then both singular and nonsingular solutions to $Q = 0$ will exist near $x = 0$ [e.g. $\phi(x) \propto x^{\pm\alpha}$]. The scheme outlined above will then fail to converge; a few iterations will yield a $\phi(x)$ which is very large near $x = 0$, jumping discontinuously to the boundary condition ϕ_L at the point $x = 0$. One can prevent the singular solution from creeping in by constraining the first three points to vary like $\phi(x) \propto x^\alpha$, replacing L_3 and K_3 in (A16) by

$$\begin{aligned} L_3 &= (\tfrac{1}{2})^\alpha = \frac{\phi(\Delta) - \phi(0)}{\phi(2\Delta) - \phi(0)} \ , \\ K_3 &= 0 \ . \end{aligned} \tag{A19}$$

More points can be constrained if desired, but three are usually enough.

Another difficulty occurs if $\phi(x) \propto x^\alpha$ with $\alpha < 1$. Here the relaxations converge, but to an answer which does not satisfy $Q_j = 0$ very well near $x = 0$. This happens because the difference equations are not accurate near a singularity of $d\phi/dx$. The problem can be avoided by making the substitution $u = x^\beta$, where $\beta \le \alpha$, so that $\phi(u) \propto u^{\alpha/\beta}$.

The Henyey relaxation method can be extended to solve a partial differential equation in x and y simply by treating $\phi(x_j, y_i)$ as distinct functions of x for each y_i. If L grid points are used in the y direction, then the matrices and vectors in (A10) and (A17) are dimensioned $M \times L$; it is clear that this method is impractical if rapid variations in y force one to choose L large. In Sec. IV the singular part of A has been factored out, so that F and ψ are slowly varying in y.

It is crucial in Sec. IV that the linearized equations (4.19) and (4.20) are solved to yield (4.21) and (4.22). These expressions must be used in place of (A19) for the region where both x and y are small. Slightly different values of a and c will result for each value of y_i, but these may be averaged and F and ψ recomputed in this region.

However, careful attention to the above points does not ensure that a satisfactory solution to the partial differential equation will be found. The difference equations resulting from (A4), (A5), and (A6) may not limit smoothly into the differential equation as $\Delta_x, \Delta_y \to 0$.[20] The equations of Sec. IV, (4.17) and (4.18), experience this problem. For example, the small-argument solution for F, (4.21), satisfies the differential equation (4.17) to fourth order in x and y. Conversion of (4.17) to a difference equation using (A5) and (A6) spoils this property; the difference equation fails to reproduce the x derivatives. A better difference equation may be derived for which

$$F = 1 - cx^2(x^2 + y^2) \tag{A20}$$

is a solution to fourth order. We introduce a new parameter $\beta(x, y)$ in the difference formula for the first derivative,

$$F_{xx}^D(x_j) \equiv \frac{1}{\Delta_x^2}(F_{j+1} - 2F_j + F_{j-1}), \tag{A21}$$

$$F_x^D(x_j) \equiv \frac{1}{\Delta_x}[\beta(F_{j+1} - F_j) + (1-\beta)(F_j - F_{j-1})] \ , \tag{A22}$$

and, writing (4.17) as

$$F_{xx} + g(x, y)F_x = h(x, y) \ , \tag{A23}$$

require that

$$(F_{xx}^D - F_{xx}) + g(x, y)(F_x^D - F_x) = 0 \tag{A24}$$

be satisfied to fourth order. This determines β,

$$\beta = -\frac{(F_{xx}^D - F_{xx}) + g(x, y)\{(1/\Delta_x)[F(x, y) - F(x - \Delta_x, y)] - F_x\}}{g(x, y)F_{xx}^D\Delta_x} \tag{A25}$$

$$= \frac{Y^4 + Y^2 + 5X^2 - 2Y^2X - 18X^3 - 11Y^2X^2 + 30X^4}{2Y^4 + 2Y^2 + 10X^2 + 22Y^2X^2 + 60X^4} \ , \tag{A26}$$

APPENDIX

The relaxation method of Henyey *et al.* (Ref. 15) is a rather general iterative scheme by which one can solve systems of ordinary differential equations with boundary conditions specified at both end points. (An extension to partial differential equations will be mentioned presently.)

Given a system of M differential equations such as

$$Q = f(x,\phi)\frac{d^2\phi}{dx^2} + g(x,\phi)\frac{d\phi}{dx} + h(x,\phi) = 0, \qquad \text{(A1)}$$

one wishes to impose boundary conditions

$$\phi(x_L) = \phi_L, \quad \phi(x_U) = \phi_U. \qquad \text{(A2)}$$

In these expressions $Q(x)$, $\phi(x)$, ϕ_L, ϕ_U, and $h(x,\phi)$ are column vectors

$$\phi(x) = \begin{pmatrix} \phi^1(x) \\ \phi^2(x) \\ \vdots \\ \phi^M(x) \end{pmatrix}, \text{ etc.,} \qquad \text{(A3)}$$

and f and g may be $M \times M$ matrices.

The equation $Q = 0$ can be converted into a set of difference equations,

$$Q_j = Q(x_j, \phi) = f(x_j,\phi_j)\left.\frac{d^2\phi}{dx^2}\right|_{x_j} + g(x_j,\phi_j)\left.\frac{d\phi}{dx}\right|_{x_j} + h(x_j,\phi_j) = 0, \qquad \text{(A4)}$$

using approximations

$$\left.\frac{d^2\phi}{dx^2}\right|_{x_j} \cong \frac{1}{\Delta^2}(\phi_{j+1} - 2\phi_j + \phi_{j-1}), \qquad \text{(A5)}$$

$$\left.\frac{d\phi}{dx}\right|_{x_j} \cong \frac{1}{2\Delta}(\phi_{j+1} - \phi_{j-1}), \qquad \text{(A6)}$$

with

$$x_j = (j-1)\Delta + x_L, \quad j = 1, N \qquad \text{(A7)}$$

$$\phi_j = \phi(x_j), \quad j = 1, N. \qquad \text{(A8)}$$

Starting with an initial guess for the solution to (A6), $\phi = \tilde{\phi}(x)$, one can improve the extent to which the $M \times N$ equations (A4) are satisfied by using Newton's method,

$$\tilde{\phi}(x_j) \to \phi(x_j) = \tilde{\phi}(x_j) + \delta\phi(x_j), \qquad \text{(A9)}$$

where $\delta\phi_j \equiv \delta\phi(x_j)$ is determined by

$$0 = Q_j + B_j\delta\phi_j + C_j\delta\phi_{j-1} + D_j\delta\phi_{j+1}. \qquad \text{(A10)}$$

The $M \times M$ matrices B_j, C_j, and D_j are given by

$$B_j^{ik} = \frac{\delta Q_j^i}{\delta\phi_j^k}, \quad C_j^{ik} = \frac{\delta Q_j^i}{\delta\phi_{j-1}^k}, \quad D_j^{ik} = \frac{\delta Q_j^i}{\delta\phi_{j+1}^k}. \qquad \text{(A11)}$$

Here and throughout the lower index refers to the point x_j and the upper indices refer to the space of functions $\phi^1, \ldots, \phi^M$. As a simple example, if

$$\phi = \begin{pmatrix} A \\ \psi \end{pmatrix}, \qquad \text{(A12)}$$

$$Q = \begin{pmatrix} \dfrac{d^2A}{dx^2} + \dfrac{1}{x}\dfrac{dA}{dx} + f(x,A,\psi) \\ \dfrac{d^2\psi}{dx^2} + \dfrac{1}{x}\dfrac{d\psi}{dx} + g(x,A,\psi) \end{pmatrix},$$

then

$$Q_j = \begin{pmatrix} A_{j+1} - 2A_j + A_{j-1} + \dfrac{\Delta}{2x_j}(A_{j+1} - A_{j-1}) + \Delta^2 f_j \\ \psi_{j+1} - 2\psi_j + \psi_{j-1} + \dfrac{\Delta}{2x_j^2}(\psi_{j+1} - \psi_{j-1}) + \Delta^2 g_j \end{pmatrix},$$

$$C_j = \begin{pmatrix} 1 - \dfrac{\Delta}{2x_j} & 0 \\ 0 & 1 - \dfrac{\Delta}{2x_j} \end{pmatrix},$$

$$D_j = \begin{pmatrix} 1 + \dfrac{\Delta}{2x_j} & 0 \\ 0 & 1 + \dfrac{\Delta}{2x_j} \end{pmatrix}, \qquad \text{(A13)}$$

$$B_j = \begin{pmatrix} -2 + \Delta^2 \dfrac{\delta f_j}{\delta A_j} & \Delta^2 \dfrac{\delta f_j}{\delta\psi_j} \\ \Delta^2 \dfrac{\delta g_j}{\delta A_j} & -2 + \Delta^2 \dfrac{\delta g_j}{\delta\psi_j} \end{pmatrix},$$

where a factor of Δ^2 has been absorbed into Q, C, B, and D.

Having disposed of these preliminaries, a description of the Henyey relaxation method is now straightforward. Since the initial guess, $\tilde{\phi}(x)$, is taken to satisfy the boundary conditions at x_L and x_U, we already know that

$$\delta\phi_1 = 0, \quad \delta\phi_N = 0. \qquad \text{(A14)}$$

But the $j = 2$ part of (A10) can now be solved for $\delta\phi_2$ in terms of $\delta\phi_3$,

$$\delta\phi_2 \equiv L_3\delta\phi_3 + K_3, \qquad \text{(A15)}$$

with

$$X \equiv \frac{x}{\Delta_x}, \quad Y \equiv \frac{y}{\Delta_x}. \tag{A27}$$

The difference formulas (A21) and (A22) are tailored for use in (4.17), and are greatly superior to (A5) and (A6).

This technique is not as successful when applied to the ψ equation (4.18). Singularities appear in the analog of (A25) corresponding to zeros of $g(y)$ and ψ^D_{yy}, and the difference formulas are not improved. As a result, derivatives of ψ are not well determined near the point $x=y=0$. Fortunately, F and its derivatives are physically more interesting than derivatives of ψ, and the F equation (4.17) decouples from (4.18) in the region where the problem occurs. A more satisfactory treatment of this problem would almost certainly have little or no effect on the results presented in Sec. IV.

*Work supported in part by the NSF under Grant No. NSF PHY 75-21590 and in part by the United States Energy Research and Development Administration.

[1]K. G. Wilson, Phys. Rev. D 10, 2445 (1974); Erice lectures, Cornell Report No. CLNS-321 (unpublished).
[2]J. Kogut and L. Susskind, Phys. Rev. D 11, 395 (1975).
[3]A. A. Migdal, Landau Institute for Theoretical Physics report, 1975 (unpublished).
[4]H. B. Nielsen and P. Olesen, Nucl. Phys. B61, 45 (1973).
[5]Y. Nambu, Phys. Rev. D 10, 4262 (1974).
[6]G. Parisi, Phys. Rev. D 11, 970 (1975).
[7]G. 't Hooft, Nucl. Phys. B79, 276 (1974).
[8]A. M. Polyakov, Zh. Eksp. Teor. Fiz. Pis'ma Red. 20, 430 (1974) [JETP Lett. 20, 194 (1974)]; Phys. Lett. 59B, 82 (1975).
[9]S. Mandelstam, Phys. Lett. 53B, 476 (1975).
[10]T. Eguchi, Phys. Lett. 59B, 73 (1975).
[11]Z. F. Ezawa and H. C. Tze, Nucl. Phys. B100, 1 (1975).
[12]E. Corrigan, D. I. Olive, D. B. Fairlie, and J. Nuyts, Nucl. Phys. B106, 475 (1976).
[13]A. Patkós, Nucl. Phys. B97, 352 (1975).
[14]See for example D. Saint-James, E. J. Thomas, and G. Sarma, *Type II Superconductivity* (Pergamon, Oxford, 1969), Chap. 3.
[15]L. G. Henyey, L. Wilets, K. H. Böhm, R. LeLevier, and R. D. Levee, Astrophys. J. 129, 628 (1959).
[16]I. Iben, Jr., in *Stellar Evolution*, edited by H. Y. Chiu and A. Muriel (MIT Press, Cambridge, Mass., 1972), p. 1.
[17]C. R. Nohl, Phys. Rev. D 12, 1840 (1975).
[18]E. Eichten *et al.*, Phys. Rev. Lett. 34, 369 (1975).
[19]A. H. Ahlberg, E. N. Nilson, and J. L. Walsh, *The Theory of Splines and Their Applications* (Academic, New York, 1967).
[20]Consistency and difference equations are discussed in R. D. Richtmyer and K. W. Morton, *Difference Methods for Initial-Value Problems* (Interscience, New York, 1957).